DOI: https://doi.org/10.24425/amm.2026.157796

I.A. PINTILIE[1], D.D.B. NERGIS[1,2], A.V. SANDU[1,2], T. FISTOS[3], P. VIZUREANU[1,2*]

THE EFFECT OF HYDROGEN PEROXIDE AND SODIUM LAURETH SULFATE CONCENTRATION ON THE MECHANICAL PROPERTIES OF FOAMED GEOPOLYMERS

To achieve the need for sustainable development and integration of a circular economy in the production of products with porous structures, the need for removing high-temperature stages and raw material consumption has increased extensively. Therefore, the aim of this study is to develop porous materials using mineral wastes as raw materials and low-energy consumption methods. Furthermore, to evaluate the effect of hydrogen peroxide and sodium laureth sulfate concentration on the mechanical properties of foamed geopolymers, different mixtures have been designed, obtained, and characterized. According to the results, the structure of geopolymer foams is significantly influenced by the activator compositions as well as by the presence of lime ash. It has also been observed that by manipulating the process parameters, geopolymer foams with controlled porosity can be produced. Moreover, the resulting geopolymer foam can be used in various fields. Due to its relatively uniform porosity and pore interconnectivity (open porosity), some mixtures with sodium dodecyl sulfate can be used for the manufacture of geopolymeric filters as they have open porosity, while some of those without this additive are suitable for the production of insulating panels for buildings as they have a compact outer surface and isolated inner pores (closed porosity).

Keywords: Coal ash based geopolymers; porous geopolymers; foams; ecofriendly materials; recycling

1. Introduction

The progressive evolution of the metallurgical industry, the high levels of coal ash, and the increasing production of mineral byproducts have become global concerns The progressive evolution of the metallurgical industry, the high levels of coal ash, and the increasing production of mineral byproducts have become global concerns [1,2]. Therefore, significant efforts are being made to find a sustainable solution for converting these wastes into new products that can substitute for conventional materials in various applications, particularly in the construction sector [3]. In the case of aluminosilicate reach byproducts, geopolymerization technology became one of the most important methods of converting these wastes into valuable materials suitable for replacing ordinary Portland cement (OPC)-based products [4,5].

The geopolymers are a sustainable solution due to their low CO_2 emissions as compared to regular Portland cement-based materials. Therefore, they have gained particular attention due to their physical and chemical properties, production methods, and low costs. Geopolymers are inorganic materials obtained by mixing two components. One of the components is a material high in aluminum and silica oxides such as metakaolin (MK), red mud (RM), fly ash (FA), rice husk ash (RHA), calcined clays, waste glass, copper mine tailings, zeolite, etc. [6,7]. The other component is an activator (an alkaline, acidic liquid component). In the case of alkaline solutions, the activator is usually based on sodium silicate, sodium hydroxide, potassium hydroxide, or potassium silicate. However, the acid activators are usually based on phosphorous acid [8].

Geopolymerization is the chemical reaction in which an oxidic material is dissolved in an alkaline solution and forms a tetragonal SI-O-Al structure after the partial removal of water. This reaction proceeds through a series of steps known as dissolution, reorientation, and solidification (see Fig. 1) [9].

The optimization of the properties of geopolymers can be obtained by proper selection of resources, the right blend, and the design of the processing to suit a particular application.

To determine the specific parameters of the raw material, activation solution and drying stage, it is necessary to take into account grain size, humidity, chemical composition, percentage between solid and liquid, proportion between sodium silicate and sodium hydroxide, concentration of sodium hydroxide

[1] "GHEORGHE ASACHI" TECHNICAL UNIVERSITY OF IASI, FACULTY OF MATERIALS SCIENCE AND ENGINEERING, PROF. D. MANGERON STREET, NO. 41, 700050, IASI, ROMANIA
[2] ROMANIAN INVENTORS FORUM, SF. P. MOVILA 3, IASI, ROMANIA
[3] NATIONAL INSTITUTE FOR RESEARCH & DEVELOPMENT IN CHEMISTRY AND PETROCHEMISTRY – ICECHIM BUCHAREST, SP. INDEPENDENTEI 202, BUCHAREST, ROMANIA
* Corresponding author:peviz2002@yahoo.com

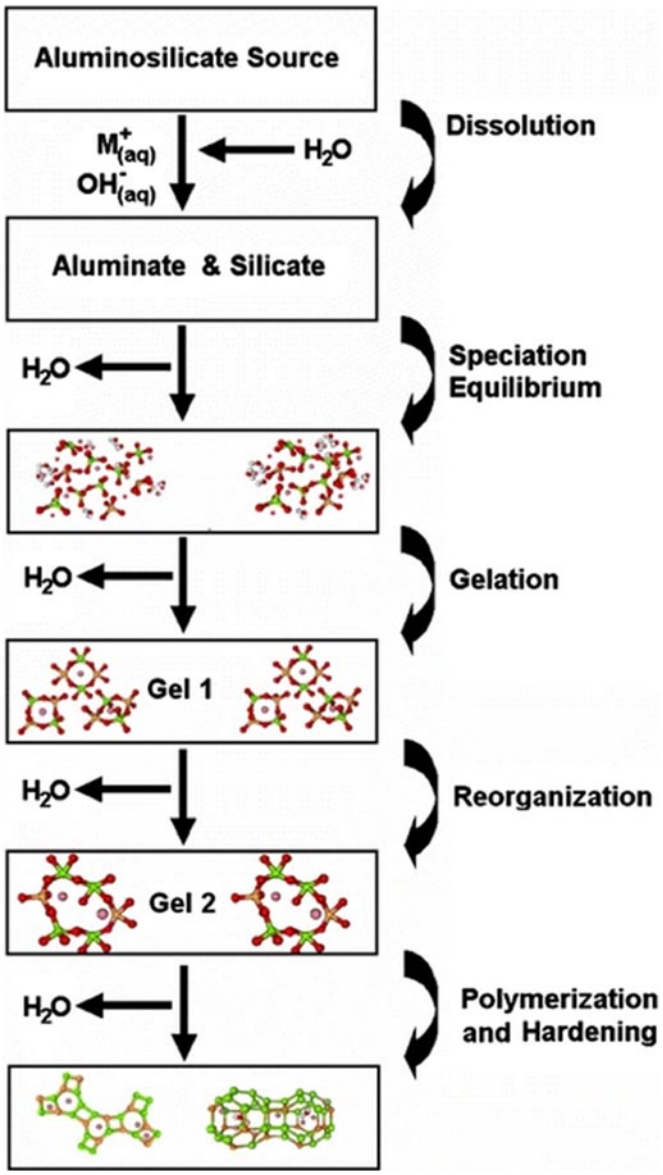

Fig. 1. The Stages of the geopolymerization process

solution, curing temperature, curing time [11]. Porous geopolymers are characterized by the purposeful addition of pores in their structure. The pore distribution, as well as the pore size, can influence the characteristics of geopolymers. In addition to properties such as physical and chemical, low CO_2 emission, and low energy consumption for manufacturing, it has a variety of applications: membranes, adsorbents, filters, catalysts, insulating materials, etc.

According to other studies, porous geopolymer foams can be obtained by four methods: self-forming method (SFM), direct foaming method (DFM), filler addition method (AFM), and particle stacking method (PSM) [12-15]. The self-forming method (SFM) produces a small, closed porosity structure without the addition of any substance. The direct foaming method (DFM) adds foaming agents or surfactants (or both) to the suspension. The resulting foam is retained inside the geopolymers, while the resulting pores are larger. By the addition-filler method (AFM), fillers or porous materials are added to the mixture.

In the particle stacking method (PSM), pores are formed by stacking the particles in geopolymer paste or between aggregate and geopolymers. The pore size is closely related to the added aggregate size [16].

Some researchers have also developed other methods of obtaining porous geopolymer foams, including suspension solidification method, direct molding method, fast microwave foaming method etc. [17].

Controllability and speed, and rapid heating are two advantages of microwave heating. The direct transfer of heat to the material via the interaction of the water molecules with the electromagnetic field is an additional advantage. Because practically any electromagnetic substance can be quickly penetrated by microwaves, the material water quickly warms up by volumetric heating and evaporates, forming a foam structure inside the object [18,19].

Graytee et al. [18] obtained geopolymer foams based on fly ash, C-type, and sodium silicate. The method used was the direct foaming method, where they used H_2O_2 as the foaming agent. They obtained samples with low density (0.24 g/cm^3) and high porosity (81.2%). The morphology is relatively uniform and the compressive strength is low (0.67 MPa).

Sayed et al. [20] examined the porosity, microstructure, and strength of the resulting geopolymers, as well as the effects of heat treatment and different additions of hydrogen peroxide used as a foaming agent. The geopolymer samples were stored in a solution that simulated bodily fluid for up to 28 days. Also, the pH levels and the weight change of the samples were analyzed to determine their biodegradability. The outcomes showed that the geopolymer foams with a high open porosity (71 vol.%), good compressive strength (3.56 ± 0.27 MPa), and appropriate chemical stability were made using 4.5 vol.% H_2O_2 and heat-treated for one hour at 500°C.

Kioupis et al. [20] evaluate the effects of synthesis parameters (type/content of foaming agent, type and concentration of alkali) on the porosity, density, and compressive strength of fly ash geopolymers made by chemical foaming. Foamed geopolymers were made with a wide range of values for pore area (3-76%), density (0.59-1.56 g/cm^3), and compressive strength (1.64-22.75 MPa).

The most commonly used foaming agent is hydrogen peroxide, which forms a porous structure. Hydrogen peroxide has a homogeneous distribution and controllable decomposition in the geopolymer suspension compared to metal powders [21,22]. Hydrogen peroxide facilitates closed porosity, but with stabilizing agents, open porous geopolymer foams can be obtained [23-25].

Finally, the properties of geopolymer foams are largely influenced by surfactants (homogeneity, grain size distribution, etc.). Therefore, by varying the quantity, types, or concentrations of surfactants while leaving the other processing parameters unchanged, it is possible to evaluate their influence on the foaming processes of geopolymers [26].

As shown in the literature, the effects of the activator and the concentrations of hydrogen peroxide and sodium laureth

sulfate on the mechanical properties and morphology of fly ash-based geopolymers have not been studied. Also, most of the publications use high temperatures to cure geopolymeric foams. Therefore, this study aims to evaluate the effect of hydrogen peroxide and sodium laureth sulfate concentration on the mechanical properties of foamed geopolymers. Accordingly, different mixtures have been designed and evaluated to obtain the optimum composition in terms of water content, hydrogen peroxide, and sodium laureth sulfate concentration.

2. Materials and methods

Any material with aluminum and silicon oxide content that an alkaline or acid activator can dissolve can become a raw material for geopolymers. Mineral wastes identified globally have the potential for geopolymerization, like thermal power plant ash, red mud, blast furnace slag, etc. In this work, two thermal power plant ash types were used to obtain the matrix and hydrogen peroxide (H_2O_2) for pore formation by the direct foaming method.

2.1. Materials characterizations

2.1.1. Fly ash

Thermal power plant ash is a by-product of coal combustion in power stations. During the burning of the coal in the furnace, the temperature in the enclosure can reach up to 1500°C; at this temperature, the non-combustible inorganic minerals (such as quartz, calcite, gypsum, gypsum, pyrite, feldspar, and various clay minerals) melted in the furnace fuse into small liquid droplets. Depending on the size of the particles, they can be blown out of the blast furnace combustion chamber by the exhaust gases and get trapped in the filters at the top of the blast furnace (fly ash), or they can end up on the furnace bottom (bottom ash). Due to the varying chemical compositions at different disposal sites, it is necessary to calculate the activation solution and the ratio of its constituents for each type of raw material. The physical, chemical, and mineralogical properties of fly ash, as well as its particle size, have a significant impact on how it behaves in geopolymers, which is why it is needed. The mineralogical and chemical composition of the particles depends mainly on the composition of the burnt coal. The characteristics of the fly ash used in this research were presented in a previous study [27].

2.1.2. Lime ashes

The second type of ash collected by CET II, Holboca, is the by-product from the desulphurization plant used [27]. This kind of waste from the desulphurization process contains hydrated calcium sulfate ($CaSO_4 - {}_2H_2O$), calcium sulfites ($CaSO_3 - 1/2H_2O$), anhydrous calcium sulfate and sulfite ($CaSO_4$ and $CaSO_3$), other calcium compounds ($Ca(OH)_2$, $CaCO_3$, $CaCl_2$), and unbound water (H_2O) mixed with fly ash and its mineral components. The water content (physically bound or free) is very low (maximum 1%), which makes the desulphurization product hygroscopic. On contact with water, they hydrate and form plaster, which hardens over time.

The activator influences the precipitation and crystallization of aluminum and silicon species present in the solution. Raw material activation is one of the most important factors in the production of a geopolymer.

When the thermal power plant ash or other material with a high aluminum content and silica is mixed with the alkaline solution, the glassy component is rapidly dissolved, but there is not enough time and space for the gel formed to pass into a fully crystalline structure. The resulting material thus has a mixed amorphous and crystalline structure.

2.1.3. Sodium silicate

Sodium silicate (Na_2SiO_3) is obtained by fusing sand (SiO_2) with sodium carbonate (Na_2CO_3) at high temperatures, followed by condensation of the product from the vapor state into a semi-viscous liquid. Due to its insufficient activation power to start the geopolymerization reaction, sodium silicate is rarely utilized as a stand-alone activator. To manufacture geopolymers based on mineral waste, a commonly found Na_2SiO_3 solution (Kynita S.R.L., Valcea, Romania) with a density of 1.52 g/cm^3 and a pH of about 11.5 will be used. According to the product quality certificate, the solution used contains min. 44.8% sodium silicate, min. 31.10% SiO_2, min. 13.70% Na_2O and additives.

2.1.4. Sodium hydroxide

The concentration and molarity of the sodium hydroxide (NaOH) solution strongly influence the final properties of the geopolymers. Beginning in the process, large concentrations of NaOH solution cause considerable resistance. NaOH-activated geopolymers are more stable in sulfated or acidic conditions and have a high crystallinity. The NaOH solution used was prepared at the concentrations preset in the recipe by dissolving commercially purchased (Kynita S.R.L., Valcea, Romania) high purity (98%) NaOH flakes in water 24 hours before use (mixing with Na_2SiO_3 and the solid component).

2.1.5. Hydrogen peroxide

Hydrogen peroxide, also known as hydrogen peroxide or perhydrol, has the chemical formula H_2O_2 and is commercially available in various concentrations (3%, 35%, etc.). H_2O_2 is a colorless liquid, soluble in ether and alcohol. In the case of geopolymers, it is used as a foaming agent, due to its property of spontaneously decomposing, resulting in water and oxygen,

to create pores of different sizes. The hydrogen peroxide used in this study has a concentration of 3%, also called pharmaceutical hydrogen peroxide, and was purchased commercially (Vitalia K SRL, Ploiesti). The hydrogen peroxide used contains 3% hydrogen peroxide, demineralized water and stabilizers (EDTA, phosphoric acid).

2.1.6. Sodium dodecyl sulfate

It is a surfactant known as SDS or Sodium Lauryl Sulfate. In the case of geopolymers, sodium dodecyl sulfate facilitates uniform mixing of the components and forms a homogeneous phase necessary for an efficient reaction. It reduces surface tensions and favors the formation of regular and uniform pore structures. Maintains suspension stability. The sodium dodecyl sulfate used in this study is an analytical reagent ($C_{12}H_{25}NaO_2S$), produced and purchased from Chemical Company S.A. (Iasi, Romania).

2.2. Foaming

A mixture consisting of sodium silicate, sodium hydroxide, fly ash, lime ash, water and hydrogen peroxide (as foaming agent) was used to produce geopolymer foams. Sodium laureth sulfate (an anionic surfactant) was also used as a pore-stabilizing agent. The mixtures studied are shown in TABLE 1.

The geopolymer foam technology flow (Fig. 2) consists of:

1. The solid component (fly ash and/or lime fly ash) is dosed and mixed for 1 minute.

TABLE 1

Composition of the studied mixtures

Mix	Na_2SiO_3 (%)	H_2O (%)	NaOH (%)	H_2O_2 (%)	FA (%)	FS (%)	SDS (%)
S1	44%	6%	2%	4%	44%	—	—
S2	44%	6%	2%	3%	39%	6%	—
S3	44%	5%	2%	5%	44%	—	—
S4	44%	5%	2%	3%	46%	—	—
S5	44%	5%	2%	3%	42%	4%	—
S6	44%	5%	2%	5%	39%	5%	—
S7	44%	6%	—	3%	47%	—	—
S8	44%	6%	—	4%	46%	—	—
S9	44%	5%	—	5%	46%	—	—
S10	35%	27%	—	3%	35%	—	—
S11	34%	27%	—	4%	35%	—	—
S12	34%	27%	—	5%	34%	—	—
S13	34%	27%	2%	3%	34%	—	—
S14	34%	27%	2%	4%	33%	—	—
S15	34%	27%	2%	5%	32%	—	—
S16	34%	26%	2%	3%	30%	5%	—
S17	34%	26%	2%	4%	29%	5%	—
S18	34%	26%	2%	5%	28%	5%	—
S19	45%	6%	—	3%	46%	—	0.05%
S20	44%	6%	—	4%	46%	—	0.05%
S21	43%	6%	—	5%	42%	4%	0.05%
S22	35%	26%	2%	3%	34%	—	0.05%
S23	34%	23%	2%	4%	37%	—	0.05%
S24	34%	23%	2%	5%	36%	—	0.05%
S25	35%	23%	2%	3%	32%	5%	0.05%
S26	34%	23%	2%	5%	31%	5%	0.05%
S27	34%	23%	2%	5%	31%	5%	0.05%

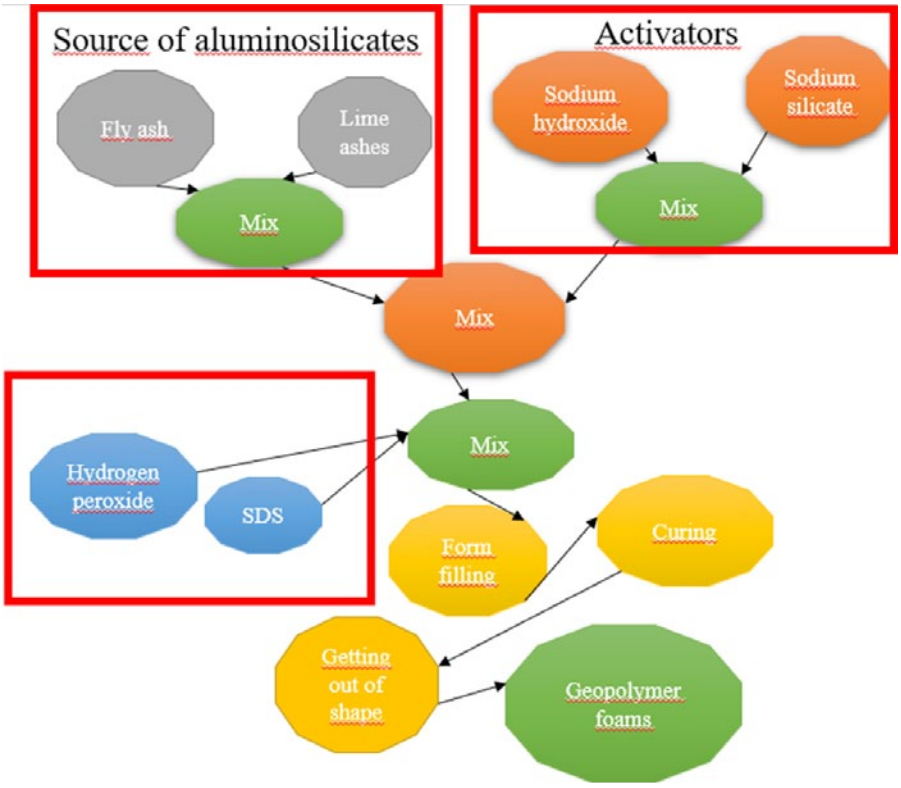

Fig. 2. Schematic representation of the technological flow of obtaining porous geopolymers

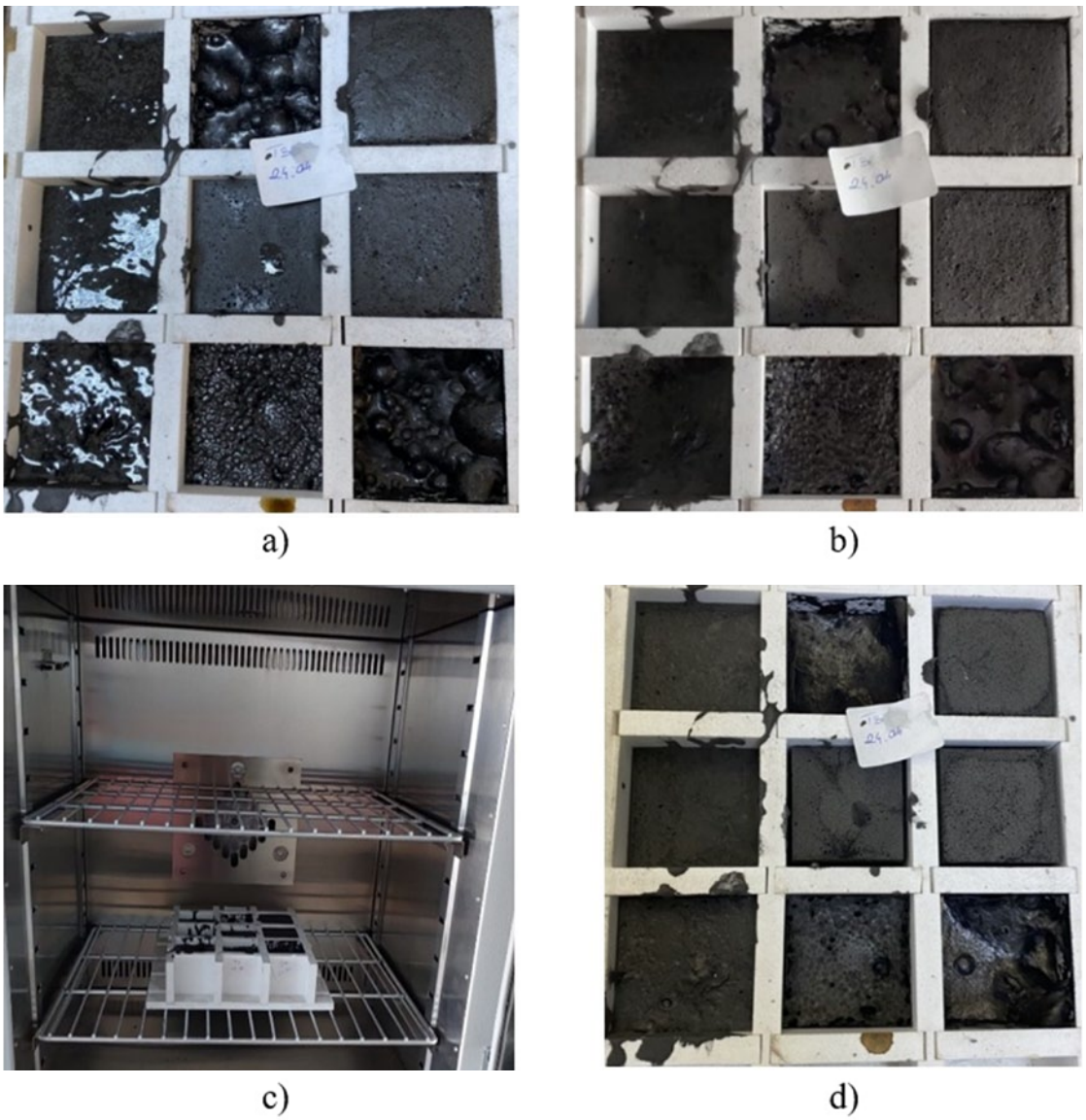

Fig. 3. Physical appearance of geopolymeric foams: a) after pouring the mixture into molds; b) after keeping at room temperature; c) after placing in the oven; d) after curing at 55°C for 24 hours

2. Add the liquid component (sodium silicate, water and/or sodium hydroxide) and mix for 1 minute. In the case of mixtures containing NaOH, NaOH was dissolved in water and then mixed with sodium silicate to obtain the activator.
3. Mix the solid component with the liquid component until homogeneous, about 5 min.
4. Add the foaming agent (hydrogen peroxide) and stir the contents for 1 minute.
5. Casting the mixture into 5 cm cube sample molds (Fig. 3a).
6. Hardening the mixture to room temperature for 24 hours (Fig. 3b).
7. Curing samples at medium temperature (55°C) in a convection oven (Fig. 3c) for 24 hours (Fig. 3d).

As can be seen (Fig. 3a, b), the amount of water and the type of ash can influence the pore distribution in geopolymers. The amount of water used plays an important role in the manufacturing process, material composition, curing conditions, and pore formation in geopolymer materials.

3. Results and discussions

In order to identify the most promising mixture for the production of geopolymer foams, the obtained samples were analyzed by stereomicroscope after the curing step at medium temperatures. According to the analysis, the following can be stated:

Sample S1 shows large pore sizes in the upper part (see top view in TABLE 2) and a very fine porosity structure in the lower part (see sectional view in TABLE 2).

Sample S2 shows small, irregularly distributed pores (see top view and side view in TABLE 2, and porosity distributed over the entire section can be observed in the inner part (see sectional view). The shrinkage is due to the high calcium content because two types of ash were used in this sample, one of them containing high amounts of calcium.

Sample S3 exhibits large pores in the upper part, visible on the sidewall (see top view and side view in TABLE 2), and a very fine porosity structure can be observed in the lower part

(see sectional view in TABLE 2). The amount of foaming agent was higher than the amount used in sample S1.

Sample S4 shows small and large pores in the upper part, which are unevenly distributed (see top view and side view TABLE 2). It resembles sample S3. A fine porosity structure is observed in the lower part, and large pores are distributed in the upper part. The amount of foaming agent was lower than in sample S3 but higher than in sample S1. In addition, samples S3 and S4 had sodium hydroxide added to the activator.

Sample S5 shows small pores, irregularly distributed in some areas (see top view and side view TABLE 2). In the side view, you can see an area of the activator that has not completely homogenized and is on the surface. Sample S5 is compositionally similar to sample S2 but different due to the foaming agent content.

Sample S6 shows small pores, irregularly distributed both on the outside (see top view, side view TABLE 2) and inside (see section view TABLE 2). The amount of foaming agent is higher than in sample S5 and the resulting porosity is more uniform in cross-section.

Sample S7 shows large, irregularly distributed pores (see top view, side view TABLE 2), and on the inside, it shows an area of fine porosity over the entire surface and large, irregularly distributed pores (see section view TABLE 2). Sodium hydroxide was not added to this sample.

Sample S8 exhibits large pores and a fine, irregular porosity structure (see side view and sectional view TABLE 2). In composition, it is similar to the S7 sample, but only the foaming agent is in higher quantity. In addition, the sample has a better structure than the S7.

Sample S9 shows large and small pores on the outside (see side view TABLE 2) and a fine porosity structure, together with large pores that are irregular. The sample is similar to S7 and S8 in composition, except for the amount of foaming agent, which is higher.

TABLE 2

Structural morphology of samples S1-S9

Mix/Sample	Top view	Side view	Section view
1	2	3	4
S1	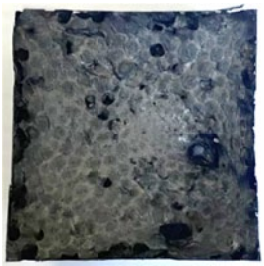	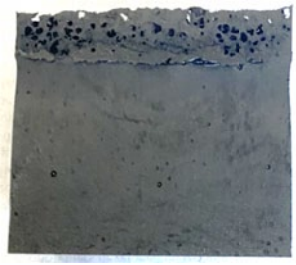	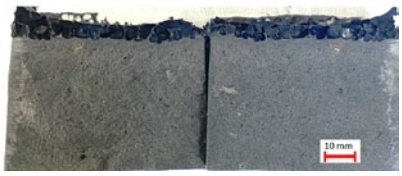
S2			
S3		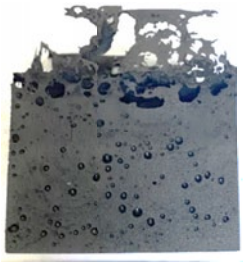	
S4		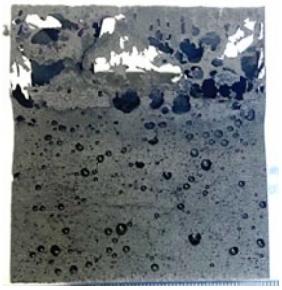	

TABLE 2. Continued

1	2	3	4
S5			
S6	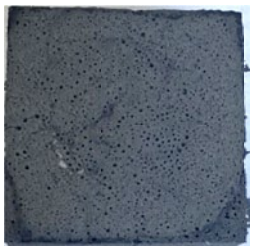		
S7		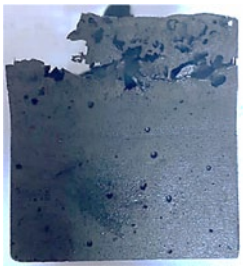	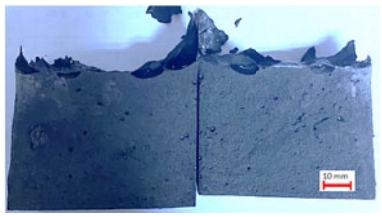
S8	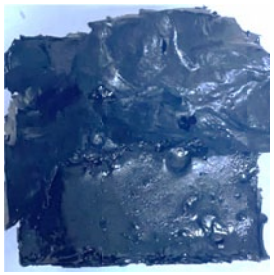		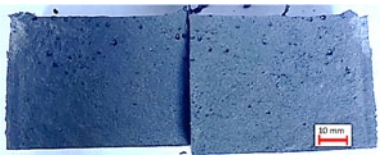
S9	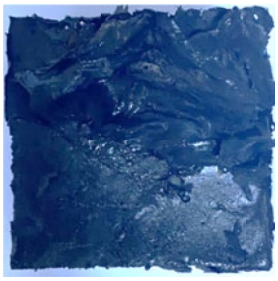		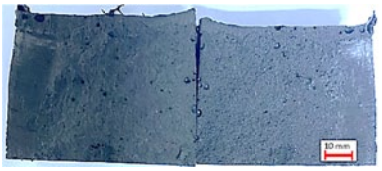

By comparing samples S1 with S2, it can be seen that by adding lime ash and introducing sodium hydroxide in the activator, the geopolymer structure is considerably modified in that the samples will no longer have a top layer with different morphology and, at the same time, the dimensional instability of the samples appears. All lime-ash samples exhibited high, nonlinear shrinkage (higher at the top of the samples).

By comparing samples S3 and S4, a similarity can be observed in terms of the top layer (see top view and side view in TABLE 2) and the inner fine porosity structure. The difference is that sample S4 has a better porosity on the outside. Although the same composition was kept in both samples, the amount of foaming agent was changed to see how it reacted. As can be seen in sample S4, there are centrally distributed small and large pores (see side view in TABLE 2).

Samples S5 and S6 exhibit porous structures, irregularly distributed on the surface but uniform in the interior (see sectional view in TABLE 2).

In structure, samples S7, S8, and S9 resemble samples S3 and S4 but differ in that sodium hydroxide has been added to samples S3 and S4.

Sample S10 shows a structure with fine porosity in some outer areas and irregular large and small pore sizes (see side view in TABLE 3). A higher porosity formed in the upper zone (see sectional view in TABLE 3) is observed in the inner part, together with small pores all over the surface.

Sample S11 shows fine porosity in the outer part, formed more in the lower zone (see side view in TABLE 3) and a compact morphology. In the sample section, small, regularly distributed pores can be observed alongside large, irregularly distributed pores.

Sample S12 shows a fine porosity structure on the outside, together with small irregular pores (see side view in TABLE 3). In cross-section, an uncontrolled porosity is observed, where large pores have formed from the central to the upper zone and smaller pores are found throughout the surface (see cross-sectional view in TABLE 3). In terms of composition, sample S12 is similar to sample S11, but the amount of hydrogen peroxide differs (more hydrogen peroxide was used in S12).

Sample S13 exhibits a fine porosity structure on the outside (see side view in TABLE 3) and a compact zone on the inside (see sectional view in TABLE 3). The liquid on the outside of the sample represents the activator expelled from the composition.

Sample S14 shows an irregular pore structure in the outer part (see side view in TABLE 3) and a compact, pore-free structure in the inner part (see sectional view in TABLE 3).

Sample S15 exhibits a fine porosity structure present in the interior (see sectional view in TABLE 3), along with larger pores in the exterior (see side view in TABLE 3).

Sample S16 shows large pores formed in the outer area (see side view in TABLE 3) and small, centrally formed pores in the lower part of the sample (see sectional view in TABLE 3).

Sample S17 shows pores of different sizes, irregularly distributed on the outside (see side view in TABLE 3). In the inner part, a fine porosity structure is observed, which is more visible than in sample S16.

TABLE 3

Structural morphology of samples S10-S18

Mix/Sample	Top view	Side view	Section view
1	2	3	4
S10	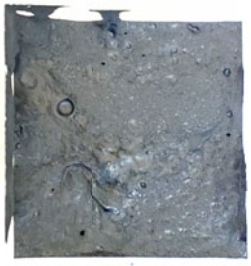	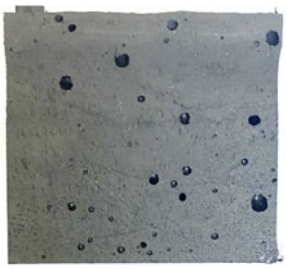	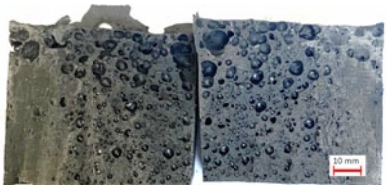
S11			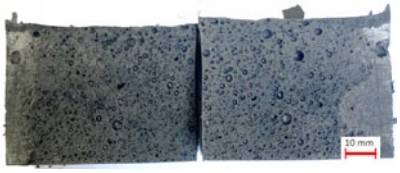
S12	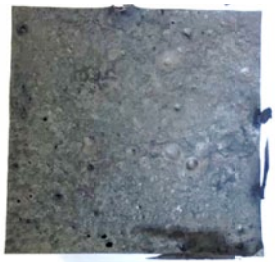	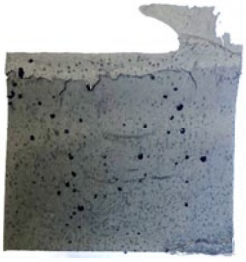	
S13		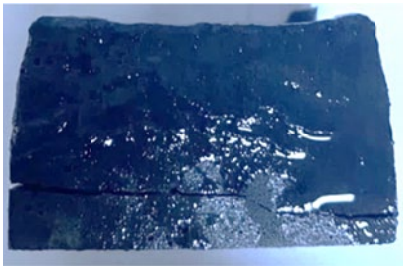	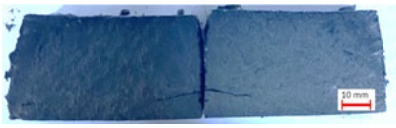

TABLE 3. Continued

1	2	3	4
S14	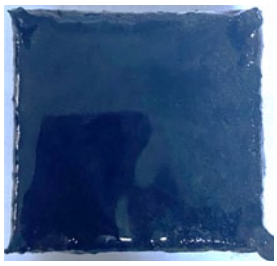	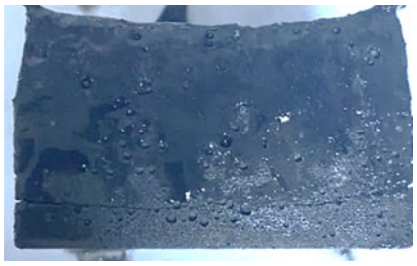	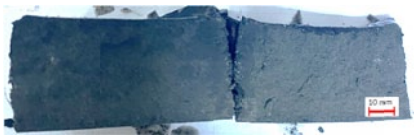
S15	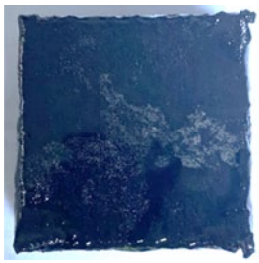	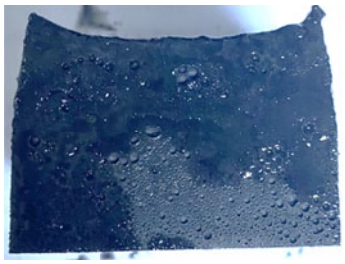	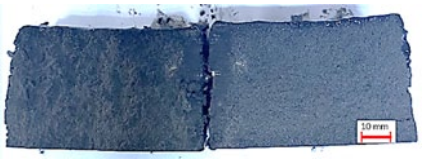
S16	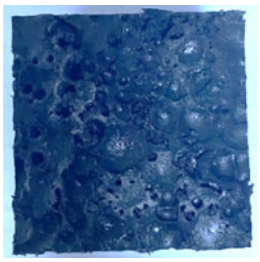		
S17			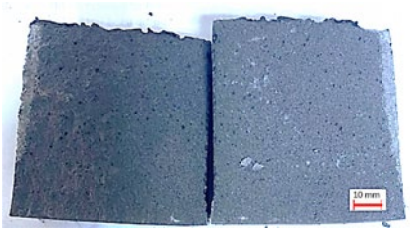
S18	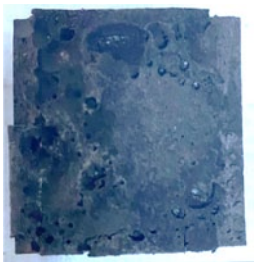		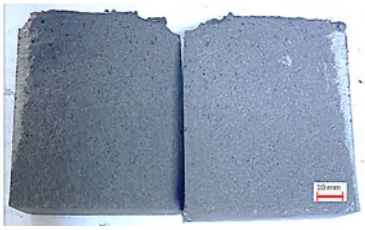

Sample S18 exhibits visible large, irregular pores in the upper area (see side view in TABLE 3), and in the inner part of the sample, the same fine porosity structure similar to S17 and S16 is observed.

By comparing samples S10 with S11, one can observe the increase in foaming agent, where a more uniform porosity was obtained in sample S11 (see section S10, S11 in TABLE 3). In sample S11, the pores remained inside the sample, which resulted in a more uniform and controlled porosity, compared to sample S10, where the pores are larger at the top, and some of the pores can be seen on the side wall.

By comparing samples S12 with S13, one can observe the influence of NaOH activator in the geopolymer structure, resulting in a compact zone on the inside and irregular pores on the outside (see section view of S13 in TABLE 3). Sample S12 shows better porosity than sample S13, as the outer and inner surfaces are porous.

By comparing samples S14 with S15, it can be seen that by raising the foaming agent quantity and increasing the amount of water, a fine porosity structure results over the entire sample surface (see side view and sectional view of S15 in TABLE 3).

By comparing the samples S16, S17, and S18, a dimensional instability of the samples can be observed due to high calcium content and high nonlinear shrinkage. All samples show fine porosity on the inside and large pores on the outside (irregular), the difference being due to the amount of foaming agent.

Sample S19 shows a thin, compact zone on the outside (see side view in TABLE 4) and a fine porosity structure on the inside, while the mechanical strength is low.

Sample S20 has the same structure as sample S19. However, the amount of foaming agent was higher than in sample S19. The pores are highlighted in this sample.

Sample S21 adhered to the walls of the mold (see top view in TABLE 4) and exhibited a fine porosity structure on the inside (see sectional view in TABLE 4) due to the increase in the amount of foaming agent and decrease in the amount of water. Even though samples S19 and S20 have the same composition, the foaming agent and the amount used play an essential role in pore formation, and this is best observed in sample S21.

Sample S22 exhibits a compact zone at the bottom and a small zone with large pores at the top (see side view in TABLE 4), and the compact zone has a fine porosity in the interior. The two zones are separated by a whitish state (soap) formed by the reaction between SDS, NaOH and H_2O_2.

Sample S23 has a similar structure to S22, except that the compact layer is thinner and the porous area larger (see sidebar in TABLE 4). The whitish layer is also visible. This difference is due to the increased quantity of foaming agents.

Compared to samples S19, S20, and S21, the dosing of the amount of water and the addition of NaOH facilitated the formation of a more favorable pore structure.

Sample S24 exhibits a porous structure and a compact surface layer at the bottom, together with the formed whitish liquid (see side view and sectional view in TABLE 4). In this sample, the addition of the foaming agent facilitated the formation of the porous structure almost all over the surface.

TABLE 4

Structural morphology of samples S19-S27

Mix/Sample	Top view	Side view	Section view
1	2	3	4
S19	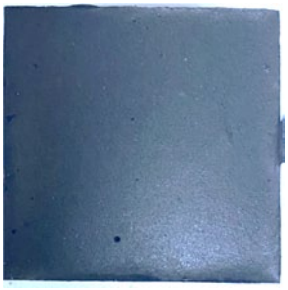	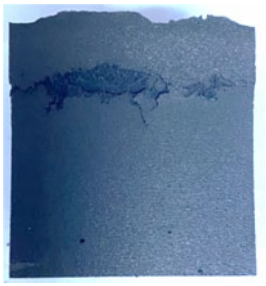	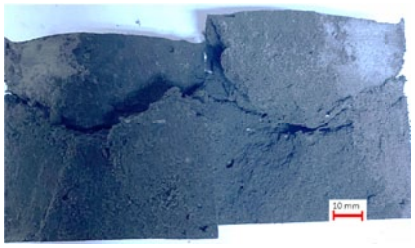
S20	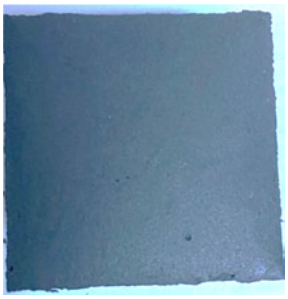	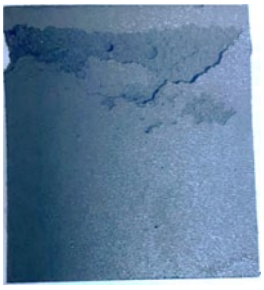	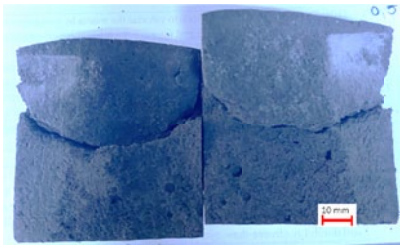
S21	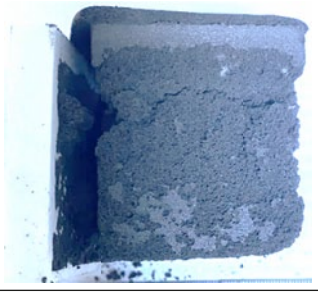		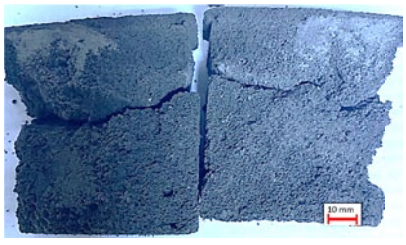
S22	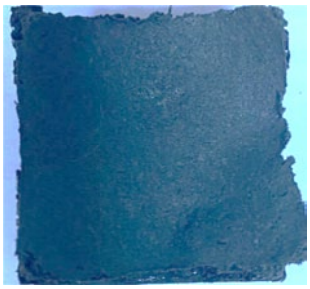	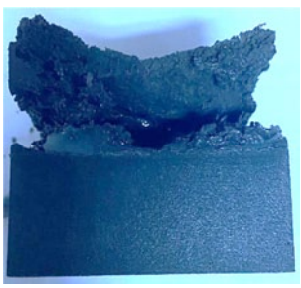	

TABLE 4. Continued

1	2	3	4
S23	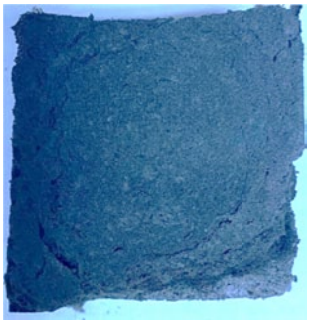	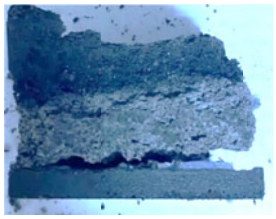	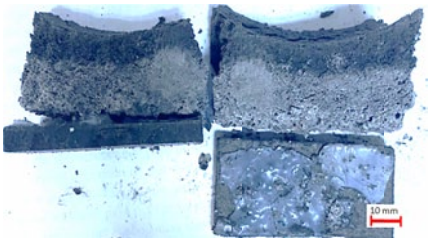
S24	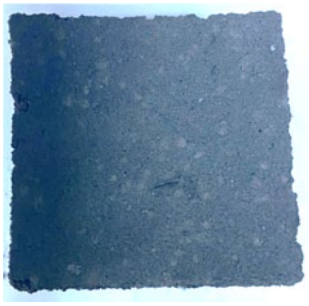	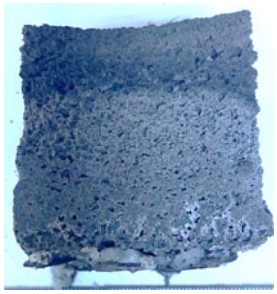	
S25	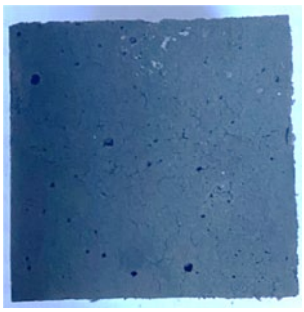	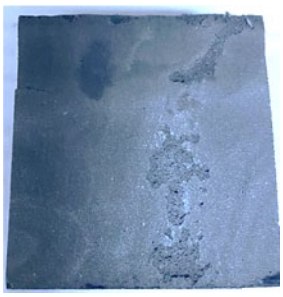	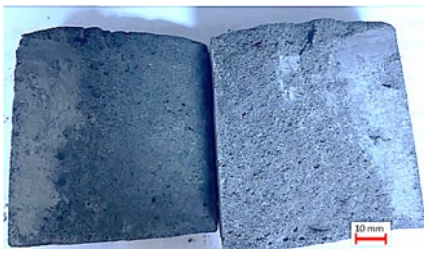
S26	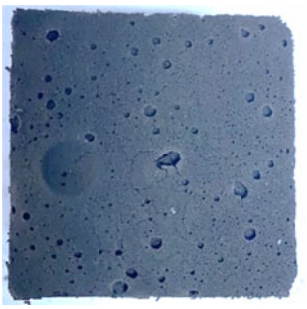	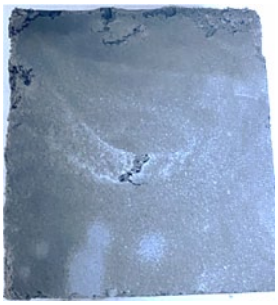	
S27	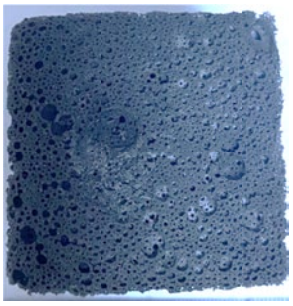		

Sample S25 exhibits a very fine, compact zone (see side view in TABLE 4) and an interior structure with fine, uniform porosity and irregularly distributed large pores (see sectional view in TABLE 4).

Sample S26 shows large pores in the upper part (see top view in TABLE 4) and a fine porosity structure in the interior, together with irregularly distributed large pores (see sectional view in TABLE 4).

Sample S27 shows a porous zone at the top (see top view and side view in TABLE 4), a finely porous structure at the bottom, and large pores formed at the top.

3.1. Mechanical properties

When examining the mechanical characteristics of the geopolymer specimens, the high concentration of defects near the mold-aggregate interface zone should be considered. Because it is specific to brittle materials, the process of breaking geopolymers goes through three phases: crack initiation, propagation of cracks, and growth and development of cracks.

One of the primary properties for evaluating the quality of geopolymer samples is compressive strength. The value obtained depends on the test conditions, specimen shape, and dimensions, manufacturing and storage conditions, loading speed, etc. Due to the friction between the surfaces of the sample and the plate, tangential stresses occur at the geopolymer-metal boundary, which prevents deformation of the sample cross-section, increasing their strength. Destruction of the specimen occurs by detachment of the lateral sides along planes inclined at approximately 30° to the vertical. The destruction mechanism during compression was also presented in previous studies [28].

Several standards specify test methods for determining the mechanical properties of geopolymer samples. Mechanical performances of the obtained geopolymers were evaluated considering the specifications of SR EN 196-1:2016.

Applying a force at the specimen's center point on its top surface while two supports hold up the bottom surface allows one to assess a specimen's bending strength (Fig. 6.), where F – load, kN; l – distance between equipment supports, mm. Except for the size and shape of the specimen, flexural strength is influenced by the same factors as compressive strength [28]. Consequently, flexural strength tests were carried out on six specimens for each mixture (three were tested at 14 days and three at 28 days) with dimensions of 40 mm × 40 mm × 160 mm. The samples that resulted from the flexural strength tests (two sectioned samples from the 40 mm × 40 mm × 160 mm sample) were further used to evaluate the compressive strength.

3.1.1. The mechanical properties of 14 days cured samples

According to the results shown in Fig. 7 and Fig. 8, samples S5 and S24 show better compressive strength, and sample S10 shows 5 times higher flexural strength.

The values of the closed porosity sample S10 indicate a relatively low compressive strength compared to the other samples. Sample S24 shows higher values compared to samples S5 and S10. Due to its open porosity, uniform pore distribution and composition, its internal structure can withstand high loads. Previous studies [29,30] also confirm the influence of pore structure and distribution on the mechanical performances of geopolymers.

Compared to sample S10, the values of sample S5 are 8% higher but 20% lower than sample S24. This indicates that its closed porosity and composition may contribute to increased strength (Fig. 4).

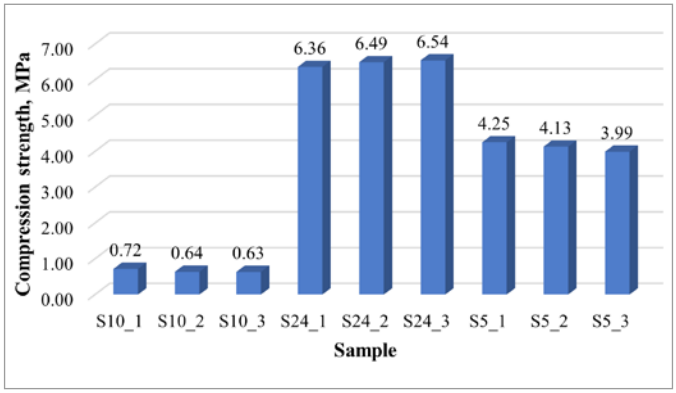

Fig. 4. Compressive strength at 14 days

Sample S10 has better flexural strength despite having lower compressive strength. Sample S24 is brittle in bending due to its rigid structure that does not allow deformation without breaking. However, the brittleness of geopolymers can be lessened by incorporating various types of fibers or additives [31,32]. Specimen S5 is similar to specimens S10 and S24, resistant to compression, but lacks the flexibility to resist flexure (Fig. 5).

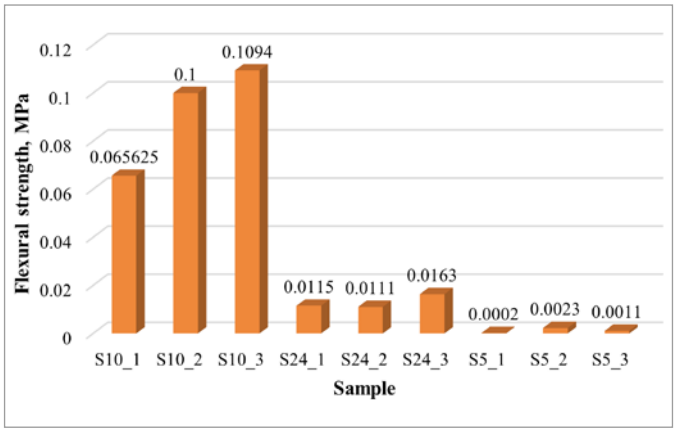

Fig. 5. Flexural strength at 14 days

The choice of the type of geopolymer foam (S5, S10, S24) should therefore depend on the application's specific requirements [33-35].

3.1.2. Experimental results at 28 days

As can be seen in Fig. 6, the samples showed an increase in compressive strength between 14 and 28 days, indicating a continuous hardening during this interval.

In both time intervals, S24 is 100% superior to S5 (36%) and S10 (8%).

Sample S10 had the highest flexural strength values at 14 and 28 days, indicating the contribution of closed porosity on the strength (Fig. 7).

The evaluation of mechanical properties by testing at 14 and 28 days is critical in evaluating the development of geopoly-

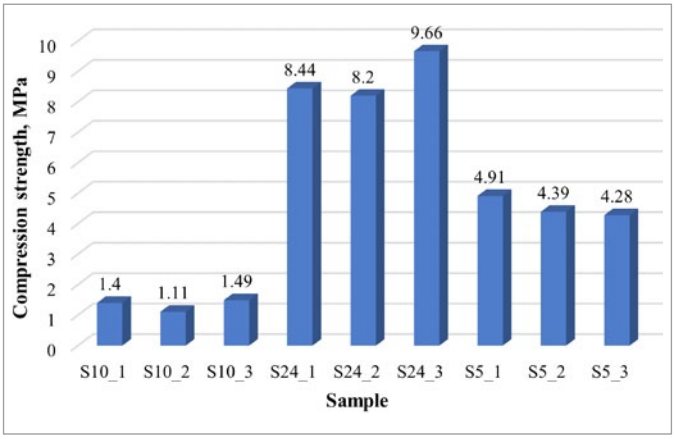

Fig. 6. Compressive strength at 28 days

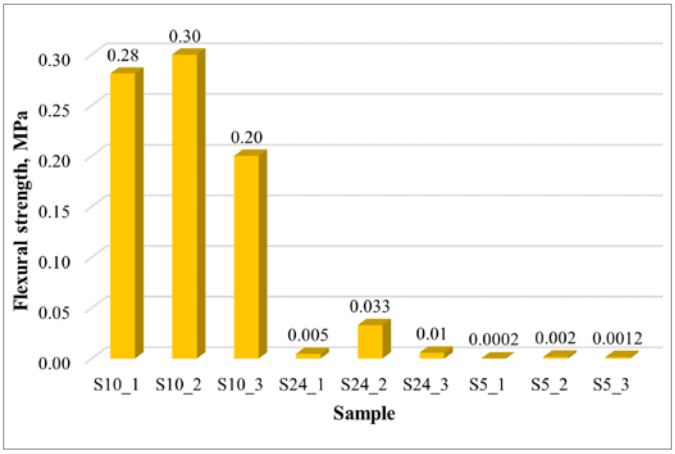

Fig. 7. Compressive strength at 28 days

mer foam [36]. The closed-porosity S10 specimen emerged as the best performer in terms of flexural strength, while the open-porosity S24 and closed-porosity S5 followed suit. The increased flexural strength over time demonstrates the importance of long-term monitoring of these materials to ensure their stability and long service life in practical applications.

4. Conclusion

This paper presents a general overview of the most common manufacturing technologies (direct foaming, incorporation of lightweight (porous) fillers, additive manufacturing, dip and impregnation method, reactive emulsion modeling method, etc.), properties (mechanical, thermal, adsorption, etc.) and corresponding applications (thermal insulation, adsorption, filtration, etc.).

Depending on the proposed use, porous geopolymer composites can have a range of mechanical, thermal and adsorption characteristics. For example, when two or more materials are mixed into a single component, changes in characteristics (mechanical, thermal, adsorption, etc.) may be obtained, expanding the variety of possible applications for composites. This is specifically the key advantage of employing composites.

Studies on porous geopolymeric foams have focused on many industrial and societally significant applications, such as the removal of organic pollutants like dyes or drugs from water, seawater desalination, photocatalysis, electromagnetic interference shielding, and a novel class of building materials (like phase change materials, thermal insulation materials, and sound insulation materials). While there is always room for more specific applications, the building sector and water treatment are two of the most promising markets for porous geopolymer composites.

According to the analysis carried out, it was observed that the most promising mixtures in terms of porosity are those specific to samples S5, S10, and S24. Therefore, the study confirms the possibility of obtaining geopolymer foams by blending S5 (34% Na_2SiO_3, 4% H_2O, 2% NaOH, 3% H_2O_2, 30% FA, 4% FS), S10 (34% Na_2SiO_3, 4% H_2O, 3% H_2O_2, 44% FA) or S24 (44% Na_2SiO_3, 33% H_2O, 2% NaOH, 5% H_2O_2, 44% FA, 0.05% SDS).

The activator compositions and the presence of lime ash significantly influence the structure of geopolymer foams. It has also been observed that geopolymer foams with controlled porosity can be produced by manipulating the process parameters.

The resulting geopolymer foams can be used in various fields. Due to its relatively uniform porosity and pore interconnectivity (open porosity), the S24 blend can manufacture geopolymeric filters. In contrast, the S10 or S5 blends are suitable for producing building insulating panels, as they have a compact outer surface and isolated inner pores (closed porosity).

Acknowledgement

This work has been carried out through the project Black Sea SIERRA Harnessing complementary curricular preparedness via sustainable management in response to civil and military pollution on the coastline, tributaries and lagoons in Black Sea's North, West, South zone, funded through the call EMFAF-2023-PIA-FLAGSHIP by the European Climate, Infrastructure and Environment Executive Agency (CINEA).

Co-funded by the European Union. Views and opinions expressed are, however, those of the author(s) only and do not necessarily reflect those of the European Union or the European Climate, Infrastructure, and Environment Executive Agency (CINEMA). Neither the European Union nor the granting authority can be held responsible for them.

REFERENCES

[1] C.R. Cánovas, G.A. Amaya-Yaeggy, D.J. Kotte-Hewa, R. Pérez-López, F. Macías, R. León, J.M. Nieto, M.D. Basallote, Exploration of biomass ashes (BA) to decontaminate highly metal-rich acid mine drainages (AMDs): Column and batch experiments. J. Clean. Prod. **489**, 144679 (2025).
DOI: https://doi.org/10.1016/j.jclepro.2025.144679

[2] G.R. Joshi, V.J. Badheka, R.S. Darji, A.D. Oza, V.J. Pathak, D.D. Burduhos-Nergis, D.P. Burduhos-Nergis, G. Narwade, G. Thiruna-

vukarasu, The Joining of Copper to Stainless Steel by Solid-State Welding Processes: A Review. Materials **15**, 15, 7234 (2022). DOI: https://doi.org/10.3390/ma15207234

[3] D. Awalluddin, M.A.M. Ariffin, M.M. Al Bakri Abdullah, N.F. Zamri, H.S. Lee, J.S. Kumar, A review of the developments in geopolymer technology. Recent Developments of Geopolymer Materials: Processing and Characterisations 3-32 (2025). DOI: https://doi.org/10.1016/B978-0-443-24068-3.00001-7

[4] I.N. Murthy, N.A, Babu, J.B. Rao, Comparative Studies on Microstructure and Mechanical Properties of Granulated Blast Furnace Slag and Fly Ash Reinforced AA 2024 Composites. Journal of Minerals and Materials Characterization and Engineering **2**, 319-333 (2014). DOI: https://doi.org/10.4236/jmmce.2014.24037

[5] G. Furtos, D. Prodan, C. Sarosi, D. Popa, M. Moldovan, K. Korniejenko, The Precursors Used for Developing Geopolymer Composites for Circular Economy – A Review. Materials **17**, 1696 (2024). DOI: https://doi.org/10.3390/ma17071696

[6] W.K. Bbosa, L. Feng, E.E. Odongol, Y. Su, T. Liu, B. Xu, Environmental sustainable treatment and disposal technologies for reservoir wastes: a review. Environmental Science and Pollution Research **31**, 59749-59766 (2024). DOI: https://doi.org/10.1007/s11356-024-35125-5

[7] M. Almokdad, R. Zentar, Assessing the environmental and technical feasibility of re-valorization of demolished road material constructed from dredged sediments. Journal of Material Cycles and Waste Management **1**, 21 (2024). DOI: https://doi.org/10.1007/s10163-024-02118-y

[8] D.P. Burduhos-Nergis, P. Vizureanu, A.V. Sandu, D.P. Burduhos-Nergis, C. Bejinariu, XRD and TG-DTA Study of New Phosphate-Based Geopolymers with Coal Ash or Metakaolin as Aluminosilicate Source and Mine Tailings Addition. Materials **15**, 202 (2022). DOI: https://doi.org/10.3390/ma15010202

[9] D.P. Burduhos-Nergis, M.M.A.B. Abdullah, P. Vizureanu, M.F. Mohd Tahir, Geopolymers and Their Uses: Review. In: IOP Conference Series: Materials Science and Engineering (2018).

[10] P. Duxson, et al., Geopolymer technology: The current state of the art. J. Mater. Sci. **42**, 2917-2933 (2007). DOI: https://doi.org/10.1007/s10853-006-0637-z/figures/15

[11] Y. Sriram, G.V.P.B Singh, Investigating the characteristics of alkali-activated fly ash lightweight blocks at lower curing temperatures. Journal of Building Pathology and Rehabilitation **10**, 1-15 (2025). DOI: https://doi.org/10.1007/s41024-024-00548-7/figures/12

[12] M. Xu, et al., Preparation of geopolymer inorganic membrane and purification of pulp-papermaking green liquor. Appl. Clay. Sci. **168**, (2019). DOI: https://doi.org/10.1016/j.clay.2018.11.024

[13] F. Colangelo, G. Roviello, et al., Mechanical and thermal properties of lightweight geopolymer composites. Cem. Concr. Compos. **86**, (2018). DOI: https://doi.org/10.1016/j.cemconcomp.2017.11.016

[14] T. Tho-In, V. Sata, P. Chindaprasirt, C. Jaturapitakkul, Pervious high-calcium fly ash geopolymer concrete. Constr. Build. Mater. **30**, (2012). DOI: https://doi.org/10.1016/j.conbuildmat.2011.12.028

[15] Z.H. Liu, Q. Tang, C.M. Li, Y.He, X.M. Cui, Preparation of NaA zeolite spheres from geopolymer gels using a one-step method in silicone oil. Int. J. Appl. Ceram. Technol. **14**, (2017). DOI: https://doi.org/10.1111/ijac.12708

[16] H. Yu, M. Xu, M. Xue, C. Chen, Y. He, Y. Cui, X. Min: A review on the porous geopolymer preparation for structural and functional materials applications. (2022).

[17] X. Li, C. Bai, Y. Qiao, X. Wang, K. Yang, P.Colombo, Preparation, properties and applications of fly ash-based porous geopolymers: A review. (2022).

[18] I. Sen, E. Dadush, D. Penumadu, Microwave-assisted foaming of expandable polystyrene beads. Journal of Cellular Plastics. **47**, (2011). DOI: https://doi.org/10.1177/0021955x10385047

[19] A. Graytee, J.G., Sanjayan, A. Nazari, Development of a high strength fly ash-based geopolymer in short time by using microwave curing. Ceram. Int. **44**, (2018). DOI: https://doi.org/10.1016/j.ceramint.2018.02.001

[20] M. Sayed, R.A. Gado, S.M. Naga, P. Colombo, H. Elsayed, Influence of the thermal treatment on the characteristics of porous geopolymers as potential biomaterials. Materials Science and Engineering C **116** (2020). DOI: https://doi.org/10.1016/j.msec.2020.111171

[21] C. Bai, T. Ni, Q. Wang, H. Li, P. Colombo, Porosity, mechanical and insulating properties of geopolymer foams using vegetable oil as the stabilizing agent. J. Eur. Ceram. Soc. **38** (2018). DOI: https://doi.org/10.1016/j.jeurceramsoc.2017.09.021

[22] Y. Qiao, X. Li, C. Bai, H. Li, J. Yan, Y. Wang, X. Wang, X. Zhang, T. Zheng, P. Colombo, Effects of surfactants/stabilizing agents on the microstructure and properties of porous geopolymers by direct foaming. Journal of Asian Ceramic Societies **9** (2021). DOI: https://doi.org/10.1080/21870764.2021.1873482

[23] X. Peng, H. Li, Q. Shuai, L. Wang, Fire resistance of alkali activated geopolymer foams produced from metakaolin and Na_2O_2. Materials **13**, (2020). DOI: https://doi.org/10.3390/ma13030535

[24] M.A. Longhi, E.D. Rodríguez, B. Walkley, Z. Zhang, A.P. Kirchheim, Metakaolin-based geopolymers: Relation between formulation, physicochemical properties and efflorescence formation. Compos. B Eng. **182** (2020). DOI: https://doi.org/10.1016/j.compositesb.2019.107671

[25] S. Petlitckaia, A. Poulesquen, Design of lightweight metakaolin based geopolymer foamed with hydrogen peroxide. Ceram. Int. **45** (2019). DOI: https://doi.org/10.1016/j.ceramint.2018.10.021

[26] V. Kočí, R. Černý, Directly foamed geopolymers: A review of recent studies. Cem. Concr. Compos. **130** (2022). DOI: https://doi.org/10.1016/j.cemconcomp.2022.104530

[27] P. Vizureanu, et all., Mechanical Performance of Coal Ash - Mine Tailings Blended Geopolymer Designed by Taguchi Method. Springer Proceedings in Materials **38**, 170-183 (2023). DOI: https://doi.org/10.1007/978-3-031-45964-1_15

[28] D.D. Burduhos Nergis, P. Vizureanu, O. Corbu, Synthesis and characteristics of local fly ash based geopolymers mixed with natural aggregates. Revista de Chimie **70** (2019). DOI: https://doi.org/10.37358/rc.19.4.7106

[29] Z. Yahya et al., Influence of Kaolin in Fly Ash Based Geopolymer Concrete: Destructive and Non-Destructive Testing. IOP Conf. Ser. Mater. Sci. Eng. **374**, 012068 (2018).
DOI: https://doi.org/10.1088/1757-899x/374/1/012068

[30] S. Chen, S. Ruan, Q. Zeng, Y. Liu, M. Zhang, Y. Tian, D. Yan, Pore structure of geopolymer materials and its correlations to engineering properties: A review. Constr. Build. Mater. **328**, 127064 (2022).
DOI: https://doi.org/10.1016/j.conbuildmat.2022.127064

[31] S. Farhan Mushtaq, et al., Effect of Bentonite as Partial Replacement of Cement on Residual Properties of Concrete Exposed to Elevated Temperatures. Sustainability **14**, 11580 (2022).
DOI: https://doi.org/10.3390/su141811580

[32] B. Vijaya Prasad, N. Anand, T. Kiran, G. Jayakumar, A. Sohliya, S. Ebenezer, Influence of fibers on fresh properties and compressive strength of geo-polymer concrete. Mater. Today Proc. **57**, 2355-2363 (2022).
DOI: https://doi.org/10.1016/j.matpr.2022.01.426

[33] I. Luharet all., Solidification/Stabilization Technology for Radioactive Wastes Using Cement: An Appraisal. Materials **16**, 954 (2023). DOI: https://doi.org/10.3390/ma16030954

[34] B. Samali, S. Nemati, P. Sharafi, M. Abtahi, Y. Aliabadizadeh, An experimental study on the lateral pressure in foam-filled wall panels with pneumatic formwork. Case Studies in Construction Materials **9** (2018).
DOI: https://doi.org/10.1016/j.cscm.2018.e00203

[35] A. Weng, et al., Study of the control and influence of humidity on the mechanical and structural properties of geopolymer foam composites based on fly ash and wood flour. Mater. Lett. **365**, 136443 (2024).
DOI: https://doi.org/10.1016/j.matlet.2024.136443

[36] D. Chen, et al., Influence of direct foaming methods on the early performance and microstructure of metakaolin-based foam geopolymers. Int. J. Appl. Ceram. Technol. **22**, e14848 (2025).
DOI: https://doi.org/10.1111/ijac.14848